Biophysical Journal
Article

Biophysical Society

Stabilizing Effect of Inherent Knots on Proteins Revealed by Molecular Dynamics Simulations

Yan Xu,[1] Shixin Li,[2] Zengshuai Yan,[2] Zhen Luo,[2] Hao Ren,[2] Baosheng Ge,[2] Fang Huang,[1] and Tongtao Yue[1,2,*]
[1]State Key Laboratory of Heavy Oil Processing and [2]Center for Bioengineering and Biotechnology, College of Chemical Engineering, China University of Petroleum (East China), Qingdao, China

ABSTRACT A growing number of proteins have been identified as knotted in their native structures, with such entangled topological features being expected to play stabilizing roles maintaining both the global fold and the nature of proteins. However, the molecular mechanism underlying the stabilizing effect is ambiguous. Here, we combine unbiased and mechanical atomistic molecular dynamics simulations to investigate how a protein is stabilized by an inherent knot by directly comparing chemical, thermal, and mechanical denaturing properties of two proteins having the same sequence and secondary structures but differing in the presence or absence of an inherent knot. One protein is YbeA from *Escherichia coli*, containing a deep trefoil knot within the sequence, and the other is the modified protein with the knot of YbeA being removed. Under certain chemical denaturing conditions, the unknotted protein fully unfolds whereas the knotted protein does not, suggesting a higher intrinsic stability for the protein having a knot. Both proteins unfold under enhanced thermal fluctuations but at different rates and with distinct pathways. Opening the hydrophobic core via separation between two α-helices is identified as a crucial step initiating the protein unfolding, which, however, is restrained for the knotted protein by topological and geometrical frustrations. Energy barriers for denaturing the protein are reduced by removing the knot, as evidenced by mechanical unfolding simulations. Finally, yet importantly, no obvious change in size or location of the knot was observed during denaturing processes, indicating that YbeA may remain knotted for a relatively long time during and after denaturation.

INTRODUCTION

Over the past decades, our understanding of protein folding has been significantly advanced by a vast number of experimental and theoretical studies (1–5). It is commonly accepted that both folding and functioning of proteins are solely determined by the unique information encoded in their amino acid sequences (6,7). However, our past knowledge on protein folding has been challenged since the discovery of knotted proteins (8,9). Given that the kinetics of knot formation is more complex and much slower than that of folding (10,11), we infer that most proteins should avoid knots during their folding. In fact, ~1% of proteins in the Protein Data Bank have been identified as containing knotted or slipknotted backbones in their native structures, and the number is still growing as development of the bioinformatic analytical method continues (12). However, a fundamental question of how a protein folds into its native state with such an entangled topological feature still remains unclear and has attracted considerable interests in recent years (13–20).

Besides folding and knotting, an equally important question to be answered is how the knotted topology is responsible for any biological functions of proteins. One noteworthy hypothesis is that knots provide additional stability necessary for maintaining the global fold and function of proteins under harsh conditions (21–23). Especially for some enzymes, the knot regions were found to directly act as or encompass the binding/active sites, prompting a speculation that knots may confer stability or rigidity to maintain catalytic properties of enzymes (24,25). Structurally, the knot region of a protein usually contains a larger number of contacts to decrease the solvent accessibility, contributing to the higher stability (26). Earlier simulations using the coarse-grained method also suggested a higher stability for proteins having knots (23). However, the molecular mechanisms underlying the stabilizing effect of knots on proteins are still far from being fully understood.

Here, we consider two proteins having the same sequence and secondary structures but differing in the presence or

Submitted June 4, 2018, and accepted for publication September 18, 2018.
*Correspondence: yuett@upc.edu.cn
Editor: Amedeo Caflisch.
https://doi.org/10.1016/j.bpj.2018.09.015

absence of a knot. One protein is YbeA, a 155-residue protein from *Escherichia coli* containing a deep trefoil knot within the sequence, and the other is the modified protein with the knot of YbeA being removed by reversing the crossing of the protein chain. After confirming that both proteins are stable under normal conditions, chemical, thermal, and mechanical denaturing results obtained from atomistic molecular dynamics (MD) simulations consistently manifest a larger stability for the knotted protein. The inherent knot restrains movement of surrounding domains to retard opening of the hydrophobic core, which is defined as a crucial step leading the protein unfolding. Once the knot is removed, both secondary and tertiary structural changes cooperatively promote the protein unfolding under denaturing conditions.

METHODS

Atomistic MD simulations with explicit solvent were performed using the GROMACS software package version 4.6.7 (27), employing CHARMM force field for the protein (28,29), together with the TIP3P model for water (30). The monomer structure of the protein named YbeA was derived from the dimer taken from the Protein Data Bank (PDB: 1NS5) (Fig. 1 *A*). The comparison structure was established by redirecting the local backbone (sequences 73–79 and 118–121) of YbeA so that only the knot was removed while other structural features were minimally perturbed (Fig. 1 *B*). The unknotted protein was referred to as YbeA*.

Several steps were conducted to prepare the simulation system for each protein. After placing the protein into a cubic box of $10 \times 10 \times 10$ nm^3 and dissolving it with 31,673 water molecules and 122 ions (62 Cl^- and 60 Na^+), the system was energy minimized using the steepest descent method to remove bad initial contacts. Then, a short simulation (10 ns) with the NVT (fixed atom number, box volume and temperature) ensemble was performed, during which the positions of carbon atoms in the protein

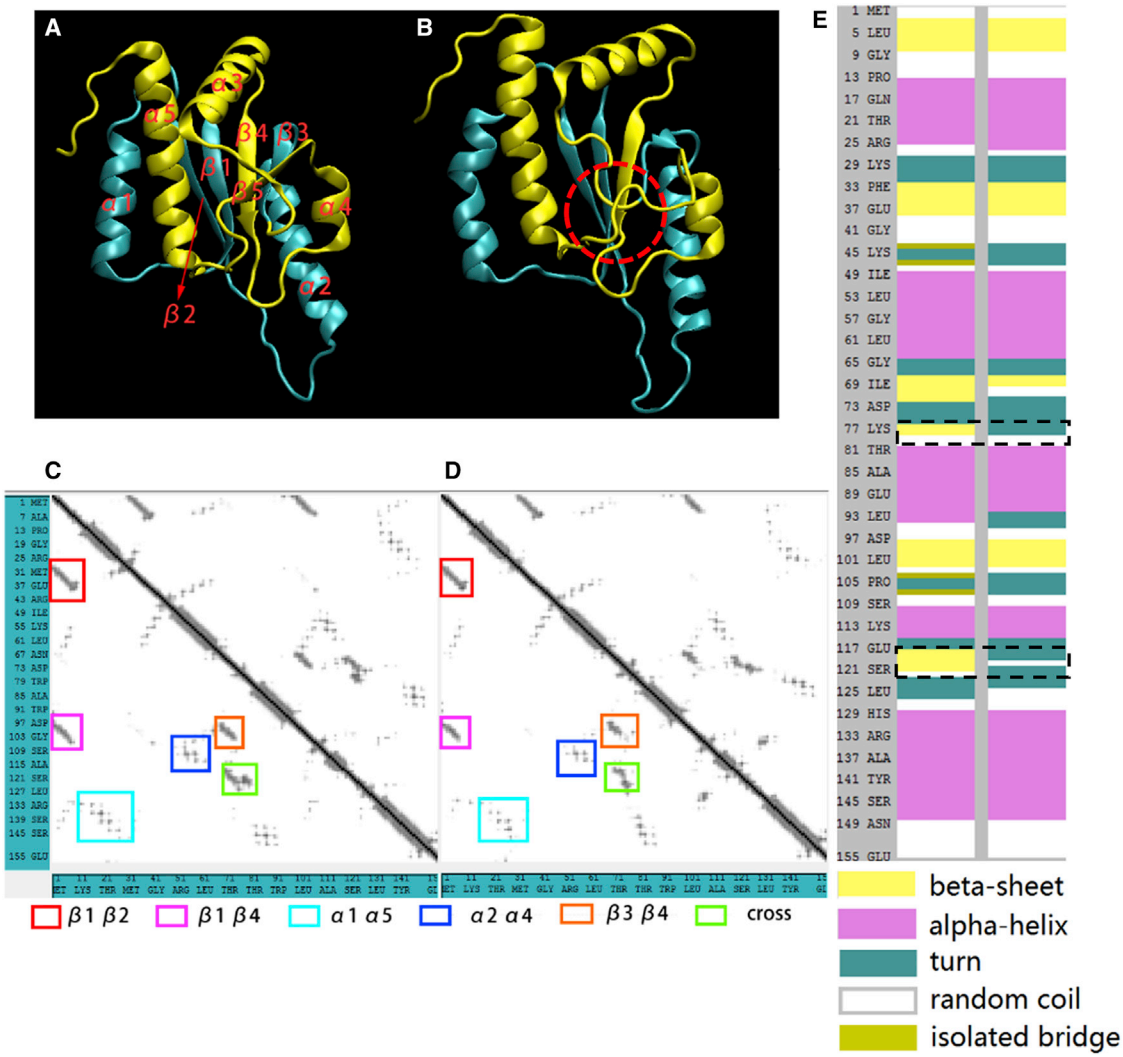

FIGURE 1 Stability of both YbeA and YbeA* under normal conditions. (*A*) The equilibrium structure of YbeA with each domain labeled. (*B*) The equilibrium structure of YbeA* with the removed knot marked by a red dashed circle. (*C* and *D*) Contact maps of both YbeA and YbeA*, which were plotted according to the distance between alpha-carbon atoms of each two residues. The graph square is colored from black linearly to gray as the distance increases from 0.0 to 10.0 Å. Several major contacts between different domains are highlighted by open squares of different colors. (*E*) The secondary structures of both YbeA and YbeA*, with minor changes labeled with black dashed squares. To view this figure in color, go online.

were restrained to let solvent fully dissolve the protein. The acquired coordinates and velocities were used as the starting point for subsequent product simulations with the NPT (fixed atom number, pressure and temperature) ensemble. Pressure and temperature were kept constant at P = 1 bar and T = 310 K using a Parrinello-Rahman barostat and the v-rescale thermostat, respectively. Electrostatic interactions were evaluated by the particle mesh Ewald summation method (31). Nonbonded interactions were truncated at a cutoff of 1.0 nm.

To accomplish chemical denaturation, a defined number of water molecules were replaced with urea to reach a concentration of 12 M (32). Thermal denaturing simulations were performed by increasing the system temperature from 310 to 520 K. Note that the denaturing conditions used in our simulations are harsher than those used in experiments. During in vitro experiments performed by Mallam and Jackson, addition of urea to a final concentration of 8 M was found to induce a complete unfolding event of YbeA (33). The midpoint of protein unfolding was measured ranging from 2.25 ± 0.02 to 2.79 ± 0.01 M, depending on the buffer condition and the protein concentration. Under such normal denaturing conditions, the observed timescale for unfolding of relatively large proteins was expected to range from tens of microseconds to milliseconds, which, however, is inaccessible to atomistic MD simulations (34,35). To shorten the unfolding time to be affordable by atomistic MD simulations, we applied the harsh conditions of higher temperature and higher concentration of urea (36). This strategy has been applied by other researchers (35) and demonstrated that simulations under harsh conditions provide results applicable to normal denaturing conditions (34). The critical temperature of TIP3P water was determined to be ~590 K (37). To perform mechanical unfolding simulations, the box size was increased to $10 \times 50 \times 10$ nm^3 to allow exerting an external force on one terminal of the protein along the y direction and avoid self-interactions of the unfolded protein with its periodic neighbors. In practice, both constant force and constant velocity protocols were used to compare the mechanical resistance of proteins with and without a knot (38). In the first mode of manipulation, a constant pulling force varying from 200 to 400 kJ/mol/nm was exerted on the C-terminus, with the N-terminus being fixed to measure the end-to-end distance. In the constant-velocity pulling manipulation, the spring constant was set to 1000 kJ/mol/nm^2 to pull the C-terminus in a constant velocity of 0.0005 nm/ps. Although the pulling rate used in our simulations was much larger than that in atomic force microscopy (AFM) experiments (39), decreasing the pulling velocity to 0.0001 nm/ps was found to produce similar results, demonstrating that our simulations can provide reasonable pictures of the overall mechanical behaviors of the proteins. Snapshots were rendered using Visual Molecular Dynamics (40).

RESULTS AND DISCUSSION

Design of an unknotted protein and stability under normal conditions

A straightforward way of elucidating the effect of an inherent knot on the protein stability is to compare a knotted protein with another protein that has nearly identical structural features other than having no knot (41,42). However, such pairs of knotted/unknotted proteins do not naturally exist, thus requiring protein engineering or molecular simulation (20). Sulkowska et al. used coarse-grained simulations to make such comparisons, albeit disregarding contributions from atomistic interactions (23,43). With computational capability being significantly improved, MD simulations at the atomistic level have become available to study the dynamics of large proteins and protein complexes (44). Here, we design a unique unknotted protein as the comparison model (YbeA*) by minimally modifying other features other than removing the knot of a knotted protein (YbeA). The design strategy is reversing the crossing segment created by parts of the backbone located at the amino acid sequences 73–79 and 118–121 (Fig. 1 *B*). To relax the protein and minimize the impact of improper contacts induced by the modification, atomistic MD simulations were performed under normal conditions for 100 ns. It was found that the native contact ratio decreased from 1.0 to 0.8 and remained nearly unchanged in the rest of the simulation time (Fig. S1 *A*). Only contacts in the vicinity of the original knot-making segments were slightly perturbed by removing the knot, whereas other contacts were nearly intact (Fig. 1, *C* and *D*). The root-mean-square deviation (RMSD) was found to increase from zero and slightly fluctuate below 0.3 (Fig. S1 *B*). The calculated root mean-square fluctuations showed similar results (Fig. S2), i.e., only the crossing segment of YbeA* fluctuated to a higher extent, whereas other segments were unperturbed. Most secondary structures remained unchanged (Fig. S1 *C*), with minor secondary structural changes occurring only for the original knot-crossing segment (Fig. 1 *E*), being ascribed to change of the local environment. Overall, both the knotted and the unknotted proteins were sufficiently relaxed and basically stable under normal conditions.

YbeA* unfolds whereas YbeA does not under a chemical denaturing condition

We compared the chemical denaturing process of YbeA with that of YbeA*. The simulation temperature was increased to 480 K to accelerate the unfolding process (35), with an important prerequisite that both proteins retained their native structures in the same simulation time by solely increasing the temperature to 480 K with no addition of urea (Fig. S3, *A–C*). Five independent simulations under the same chemical denaturing conditions were performed for each protein. Notably, in the presence of urea, YbeA* was fully denatured, as characterized by striking increases of the RMSD (Fig. 2 *A*) and rapid decreases of the native contact ratio (as determined based on the van der Waals radii of heavy atoms) from 1.0 to nearly 0.0 in less than 80 ns (Fig. 2 *B*) (45,46). By contrast, slighter increases of the RMSD were observed for YbeA (Fig. 2 *A*), and at least 20% and up to 50% of native contacts in YbeA were preserved after 100 ns simulations (Fig. 2 *B*), suggesting a partial unfolding transition.

A typical simulated denaturing process of YbeA* was analyzed as follows (see Figs. S4 and S5 for unfolding pathways of both YbeA and YbeA* in all five independent simulations). Note that the pathway of protein unfolding can be not unique and influenced by the order of contacts being broken under different denaturing conditions (16). Once the order is changed, some geometrical constraints may be generated to alter the subsequent unfolding progress (47).

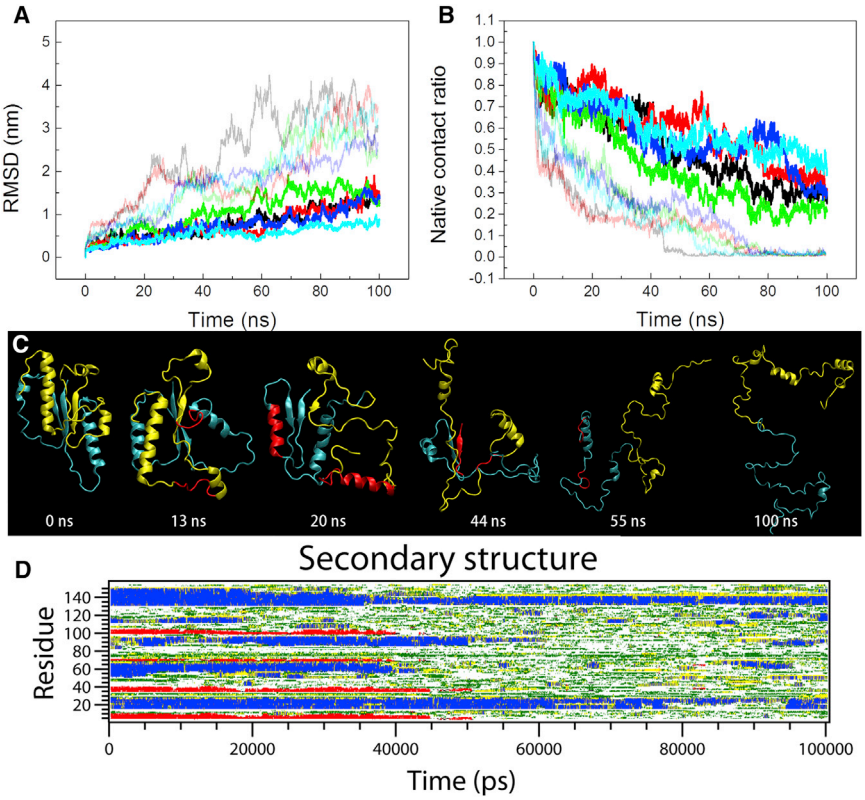

FIGURE 2 Comparing stability of YbeA with YbeA* under the same chemical denaturing conditions. (*A*) Time evolutions of the RMSD for both proteins in five independent simulations. Lines for YbeA* are set at semitransparent for ease of comparison with YbeA. (*B*) Time evolutions of the native contact ratio for both proteins in five simulations. (*C*) The time sequence of typical snapshots depicting unfolding of YbeA*, with the major secondary structural changes at each step being colored with red. (*D*) The time evolution of the secondary structural change of YbeA*. The system temperature is increased to 480 ns to accelerate protein unfolding. The urea concentration is 12 M. To view this figure in color, go online.

Shown in Fig. 2 *C* is the time sequence of typical snapshots depicting a typical unfolding pathway of YbeA* extracted from five independent simulations. In detail, the structural change of YbeA* started from the crossing segment at 13 ns, being followed by a separation between α1 and α5 helices. Crucially, such a separation opened the hydrophobic core consisting of four β-sheets exposed in water. Shortly, the four β-sheets were sequentially unfolded and separated from each other (44 ns). Finally, the polypeptide chain was fully denatured and expanded randomly in the simulation box (100 ns). We monitored the secondary structural changes of YbeA and YbeA* and found that most secondary structures of YbeA* were lost in 50 ns (Fig. 2 *D*), whereas those of YbeA were nearly unperturbed in the same simulation time (Fig. S3 *D*). Notably, in all five independent simulations, the separation between α1 and α5 helices, which was identified as a crucial step initiating the protein unfolding, occurred for YbeA*at ~30 ns, whereas for YbeA it occurred later, after 80 ns.

We calculated interaction energies between proteins and solvent, including water and urea molecules (Fig. S6 *A*). A very slight decrease of the interaction energy was observed for YbeA, suggesting a higher resistance against urea denaturation. Nearly no urea molecules were found to enter the hydrophobic region of YbeA to play the denaturing role (Fig. S6 *B*). By contrast for YbeA*, the interaction energy was initially lowered by removing the knot. Nevertheless, it remained nearly unchanged in the absence of urea (Fig. S6 *C*). After replacing water with 12 M urea, strikingly, the interaction energy rapidly decreased, suggesting a denaturing role played by urea molecules. Accordingly, several urea molecules were found to immediately enter the hydrophobic core at 20 ns upon separation between α1 and α5 to further denature the protein (Fig. S6 *D*).

Both YbeA and YbeA* unfold under enhanced thermal fluctuations

The system temperature was further increased to 520 K with the expectation that proteins can be denatured under enhanced thermal fluctuations (48). Shown in Fig. 3 are time evolutions of the native contact ratios calculated for both proteins. They finally decreased from 1.0 to ~0.1 at the end of 100 ns simulations, suggesting that both proteins were thermally denatured. However, both pathway and rate of the protein unfolding were quite different. Strikingly, the unfolding of YbeA* was completed in 20 ns, whereas that of YbeA was much slower and seemingly stepwise, indicating that several barriers may exist during the denaturing process of YbeA, due to prescence of the inherent knot.

A typical unfolding pathway of YbeA extracted from multiple independent simulations is depicted in Fig. 4. Notably, the unfolding of YbeA started preferentially from the domain α2 at 19 ns (Fig. 4 *A*), being accompanied by a sudden decrease of the native contact ratio (Fig. 3) and an increase of the RMSD (Fig. S7). Once the domain was

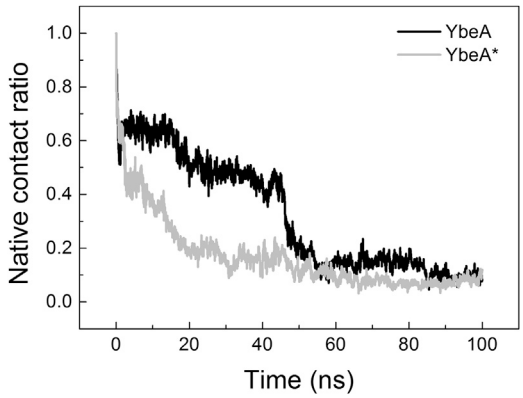

FIGURE 3 Time evolutions of the native contact ratios for YbeA (*black*) and YbeA* (*gray*) under enhanced thermal fluctuations. The system temperature was further increased to 520 K, under which both proteins were found to unfold, although at different rates and with distinct pathways.

unraveled, its constraint on the neighboring domain α4 was reduced, thus enhancing domain fluctuations of the near-knot region (Fig. S7). As a consequence, domain α5 separated from α1 at 46 ns to open the hydrophobic core, similar to the chemical denaturation of YbeA* (Fig. 2). Then, water molecules immediately entered the hydrophobic core to further unfold the four β-sheets at 50 ns (Fig. S8). Finally, only several short α-helical fragments were partly retained and confined around the knot position (Fig. 4, *A* and *B*). The tertiary structural change was further characterized by the sequence of the contact map (Fig. 4 *C*). As is seen, most tertiary structures were sequentially perturbed, finally leaving the knot region separating from the unknotted region and swaying in the rest of the simulation time (Fig. 4, *A* and *C*). Neither knot loosening nor slipping toward either direction was observed during the thermal denaturation process (Fig. S9), at least in the finite simulation period, indicating that specific interactions may exist to preserve the knot structure. This observation was consistent with previous experimental findings that proteins remained knotted under strongly denaturing conditions, supporting an important viewpoint that threading occurs early in folding reactions of knotted proteins (16,49,50). However, there exist other experimental and simulation studies reporting that the knot can be untied after long time periods of denaturation (51), pointing to the opposite view that the knot is acquired in later stages of protein folding (9,47).

Under the same thermal denaturing condition, by contrast, the unfolding of YbeA* was more rapid and occurred from a more striking tertiary structural change of the crossing segment (Fig. S10 *A*). The same crucial separation between α1 and α5 occurred earlier at 20 ns because of the absence of the knot restraint. Shortly, secondary structures of β1, β4, and β2 were sequentially perturbed (Fig. S10 *B*). Finally, the denatured protein was tangled like a twine ball with nearly no native contact being preserved (Fig. S10 *C*; Fig. 3).

Fig. 5 shows two time-event lines illustrating the distinct unfolding pathways of YbeA and YbeA*. In particular, the inherent knot can geometrically restrain the tertiary structural change of YbeA, whereas YbeA* is readily denatured without the restraint of the knot. Thus, the unfolding of YbeA was initiated by a secondary structural change occurring for the domain α2 (19 ns), followed by trivial structural undulations under thermal fluctuations, until the domain α1 separated with α5 (46 ns) to accelerate unfolding of the four β-sheets composing the hydrophobic core (50–80 ns). Once the protein was denatured, the knotted region was separated from the protein and kept swinging as an integral. The distinct unfolding pathway was for YbeA*, which first underwent a local tertiary structural change (cross separating at 5 ns). With the topological restraint being removed, the same event of α1-α5 separation occurred earlier (20 ns) than YbeA (46 ns). Shortly, the entire protein was fully denatured with nearly no barriers. Finally, the more striking tertiary structural change of YbeA* induced the protein collapse to form a disordered structure (100 ns), different from the chemical denaturing process, in which the fully denatured YbeA* was loosely extended because of interactions with urea molecules (Fig. 2).

Stretching manipulations manifest a higher mechanical stability for YbeA

Another effective way to examine the stability of a protein is performing mechanical manipulations, such as stretching. In experiments, mechanical stretching can be manipulated using AFM (52), acquiring the force-extension curves to analyze mechanical resistance of proteins. However, interpreting the experimentally measured force spectrum at the molecular level is still difficult, thus requiring the assistance of atomistic MD simulations (38,53). One can expect that the knotted protein YbeA has a higher resistance against the mechanical stretching (54). To test it, we performed mechanical unfolding simulations in which an external force was exerted on the C-terminus, with the N-terminus being fixed to probe the mechanical resistance against the stretching. Two modes of manipulation were applied for better comparison. One is exerting a constant force, and the other is pulling in a constant velocity. Accordingly, evolutions of the end-to-end distance and the resistance force, respectively, can be monitored. As proved by He et al., the mechanical unfolding pathway can be not unique but may experience several different intermediate states (38). Here, for each mode of manipulation, multiple independent simulations were performed to identify a typical unfolding pathway that coincides with that under thermal and chemical denaturing conditions.

In the first mode of manipulation, a constant force of 400 kJ/mol/nm was exerted on the C-termini of both YbeA and YbeA* to get evolutions of the end-to-end distance (Fig. 6 *A*). Apparently, mechanical stretching on

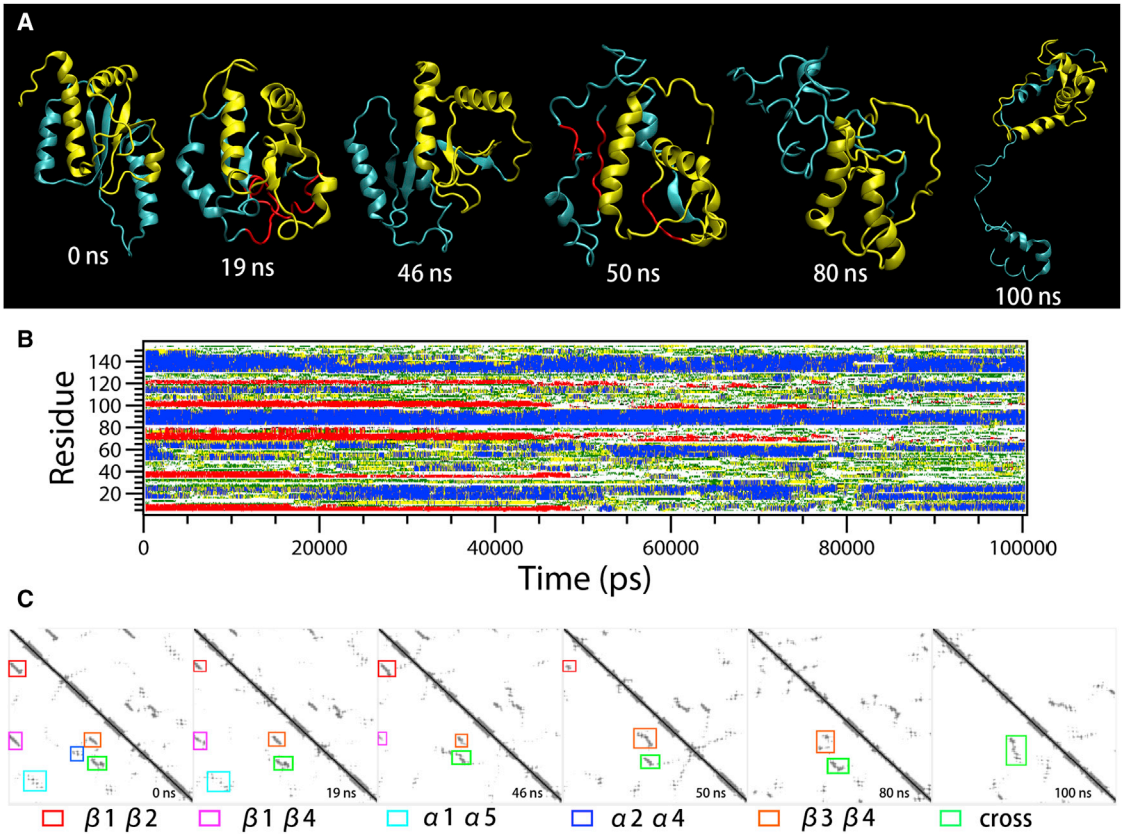

FIGURE 4 Unfolding of YbeA under a higher temperature of 520 K. (*A*) The time sequence of typical snapshots with the secondary structural changes at each step colored with red. (*B*) The time evolution of the secondary structural changes. (*C*) The time sequence of the contact map. To view this figure in color, go online.

YbeA was more difficult than that on YbeA*, manifesting a higher stability for YbeA. In detail, three plateaus during stretching on YbeA were identified, being respectively associated with the β1-β4 separation, the β1-β2 separation, and the knot-tightening events (Fig. 6 *C*) Note that each plateau may suggest an intermediate state because several energy barriers exist retarding the mechanical unfolding of proteins (53). Besides the hydrophobic interactions and hydrogen bonds formed among β-sheets that may contribute to the energy barriers for stretching (Fig. S11), the existence of the knot was inferred to provide additional restraint to retard the mechanical unfolding. By removing the knot, such barriers were effectively reduced, as reflected by a more rapid increase of the extension of YbeA* than that of YbeA.

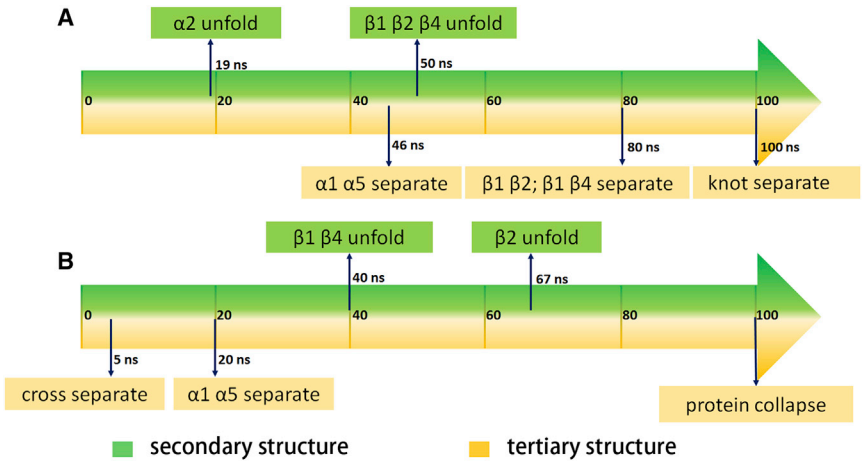

FIGURE 5 Schematic illustration of different unfolding pathways for YbeA (*A*) and YbeA* (*B*). To view this figure in color, go online.

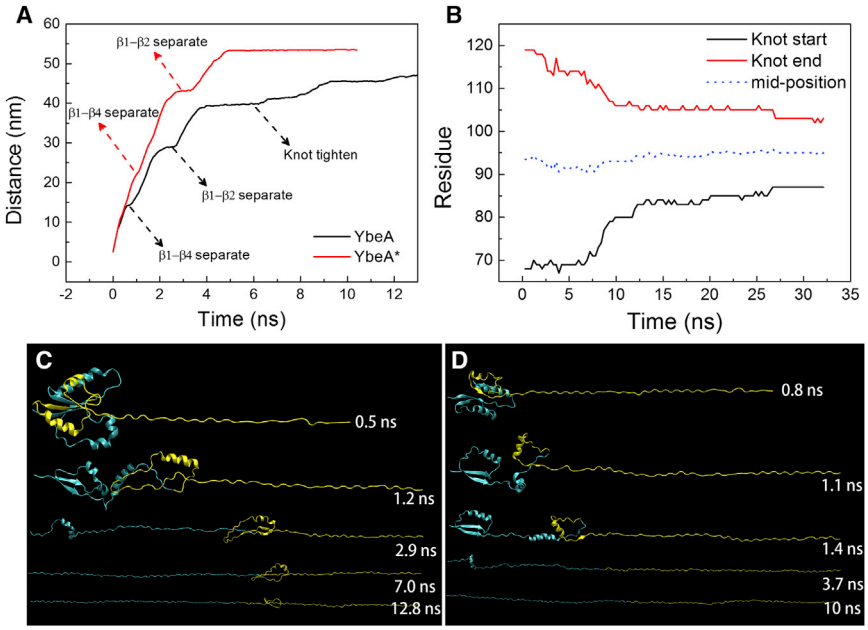

FIGURE 6 Mechanical stretching on two proteins with a constant force of 400 kJ/mol/nm. (*A*) Time evolutions of the end-to-end distances for YbeA (*black*) and YbeA* (*red*). (*B*) Sequential movement of two knot termini and mid-position for YbeA during the knot-tightening process. (*C* and *D*) Time sequences of typical snapshots showing mechanical unfolding processes of YbeA (*C*) and YbeA* (*D*). To view this figure in color, go online.

Especially for YbeA, separation of the β-sheet domains was accompanied by a separation between the knotted region and the unknotted region (Fig. 6 *C*), in agreement with the results of the thermal denaturing process (Fig. 4). We calculated the knot change using the KMT algorithm (55,56) and found that both size and location of the knot did not change until all β-sheets were separated. After that, the knot was gradually tightened but with the mid-position being nearly unchanged, manifesting specific interactions stabilizing the knot (Fig. 6 *B*). Finally, both proteins were fully denatured with the knot of YbeA being tightened into 16 residues (Fig. 6, *B–D*), similar to that measured for two other trefoil-knotted proteins, YibK and MJ0366 (57,58).

The above pulling simulations did not capture the crucial step of α1-α5 separation as identified in thermal denaturing simulations (Fig. 4) partly because the overlarge pulling force rapidly stretched the protein to be hastily denatured, with potential intermediate states being avoided. We decreased the pulling force to 200 kJ/mol/nm to reduce the rate of stretching. As expected, a gradual separation between α1 and α5 was observed, accompanied by several steps of breaking the hydrophobic interactions between Val^{16}, Phe^{20}, Leu^{24}, and Phe^{27} in the α1 domain and Leu^{131}, Val^{132}, Val^{134}, Leu^{135}, Val^{136}, Ala^{137}, Leu^{140}, and Ile^{146} in the α5 domain (Fig. S12 *A*). Although only the step of α1-α5 separation was achieved in the limited simulation time because of the decreased pulling force, the higher stability for YbeA can be evidenced by the different rate and extent of mechanical unfolding. The final end-to-end distance of YbeA was 14 nm, whereas that of YbeA* was 20 nm without restraint of the knot (Fig. S12 *B*). For both proteins, no separation of β-sheets was observed (Fig. S12, *C* and *D*), suggesting that both the pathway and the extent of the mechanical protein unfolding are affected by the external stretching force.

We next considered constant speed stretching on YbeA and YbeA*. The pulling velocity was set as 0.0005 nm/ps with the spring constant fixed at 1000 kJ/mol/nm^2. In this mode of manipulation, we got the resistance force as a function of time (Fig. S13). Although the current velocity used in our simulations was larger than that in AFM experiments (59), using different pulling velocities in both AFM experiments (50–4000 nm/s) and mechanical MD simulations (0.00025–0.05 nm/ps) was found to generate similar results of the unfolding pathways of the slipknotted protein AFV3-10 (53), demonstrating that major features of mechanical unfolding of our proteins should be preserved. Again, two proteins showed distinct mechanical unfolding pathways, as reflected by both the structural changes and evolutions of the resistance force. The first force peak at 18 ns for YbeA was due to separation between α1 and α5, being followed by two major peaks corresponding to separations between β1 and β4 (30 ns) and β1 and β2 (55 ns), respectively. After that, the knot was gradually tightened to further increase the resistance force in the late simulation time. In contrast, for YbeA*, the early force peak reflecting separation between α1 and α5 was reduced, suggesting easier unfolding without the knot. Furthermore, opening the hydrophobic core via separations of β-sheets was found to occur in a shorter time interval. Finally, both proteins were denatured and fully expanded in the simulation box.

CONCLUSIONS

In summary, we have combined unbiased and mechanical atomistic MD simulations comparing chemical, thermal,

and mechanical unfolding properties of two proteins—one of which contains an inherent knot (YbeA), whereas the other does not (YbeA*)—to reveal the stabilizing effect of inherent knots on proteins. Both proteins are stable under normal conditions, whereas only YbeA* unfolds when transferred into a 12 M urea solution. Under enhanced thermal fluctuations, both proteins unfold but at different rates and with distinct pathways. Opening the hydrophobic core via separation between two α-helices is a crucial step leading the protein unfolding, which, however, is restrained for the knotted protein by topological and geometrical frustrations. Energy barriers for denaturing the knotted protein can be reduced by removing the knot, as revealed by mechanical unfolding simulations. Both the size and the location of the knot are nearly unchanged during the finite period of unfolding simulations, indicating that the protein YbeA may remain knotted for a relatively long time during and after denaturation. Equivalently, threading the protein terminal across a twisted loop may occur early in the folding reaction of YbeA. However, this hypothesis may not apply to other knotted proteins, especially for those containing shallow knots or slipknotted conformations. This research can pave the way toward investigating relations between protein folding and protein functioning.

SUPPORTING MATERIAL

Thirteen figures are available at http://www.biophysj.org/biophysj/supplemental/S0006-3495(18)31067-1.

AUTHOR CONTRIBUTIONS

Y.X., F.H., and T.Y. designed the research. Y.X. performed MD simulations. Y.X., S.L., Z.Y., Z.L., H.R., B.G., F.H., and T.Y. analyzed data. Y.X., S.L., F.H., and T.Y. wrote the manuscript.

ACKNOWLEDGMENTS

We are grateful for financial support from the Science and Technology Major Project of Shandong Province (2016GSF117033), the Natural Science Foundation of Shandong Province (ZR2018MC004), and the Qingdao Science and Technology Project (16-5-1-73-jch). This work was also partly supported by the National Natural Science Foundation of China (21573289 and 21673294) and the Fundamental Research Funds for the Central Universities. Simulations were performed at the National Supercomputing Center in Shenzhen.

REFERENCES

1. Dobson, C. M. 2003. Protein folding and misfolding. *Nature.* 426:884–890.
2. Reddy, G., Z. Liu, and D. Thirumalai. 2012. Denaturant-dependent folding of GFP. *Proc. Natl. Acad. Sci. USA.* 109:17832–17838.
3. Schaeffer, R. D., A. Fersht, and V. Daggett. 2008. Combining experiment and simulation in protein folding: closing the gap for small model systems. *Curr. Opin. Struct. Biol.* 18:4–9.
4. Gething, M. J., and J. Sambrook. 1992. Protein folding in the cell. *Nature.* 355:33–45.
5. Onuchic, J. N., and P. G. Wolynes. 2004. Theory of protein folding. *Curr. Opin. Struct. Biol.* 14:70–75.
6. Rose, G. D., P. J. Fleming, …, A. Maritan. 2006. A backbone-based theory of protein folding. *Proc. Natl. Acad. Sci. USA.* 103:16623–16633.
7. Haber, E., and C. B. Anfinsen. 1961. Regeneration of enzyme activity by air oxidation of reduced subtilisin-modified ribonuclease. *J. Biol. Chem.* 236:422–424.
8. Taylor, W. R. 2000. A deeply knotted protein structure and how it might fold. *Nature.* 406:916–919.
9. Wallin, S., K. B. Zeldovich, and E. I. Shakhnovich. 2007. The folding mechanics of a knotted protein. *J. Mol. Biol.* 368:884–893.
10. Mallam, A. L., E. R. Morris, and S. E. Jackson. 2008. Exploring knotting mechanisms in protein folding. *Proc. Natl. Acad. Sci. USA.* 105:18740–18745.
11. Sułkowska, J. I., J. K. Noel, and J. N. Onuchic. 2012. Energy landscape of knotted protein folding. *Proc. Natl. Acad. Sci. USA.* 109:17783–17788.
12. Virnau, P., A. Mallam, and S. Jackson. 2011. Structures and folding pathways of topologically knotted proteins. *J. Phys. Condens. Matter.* 23:033101.
13. Faísca, P. F. 2015. Knotted proteins: a tangled tale of structural biology. *Comput. Struct. Biotechnol. J.* 13:459–468.
14. Ziegler, F., N. C. Lim, …, M. Rief. 2016. Knotting and unknotting of a protein in single molecule experiments. *Proc. Natl. Acad. Sci. USA.* 113:7533–7538.
15. Lim, N. C., and S. E. Jackson. 2015. Mechanistic insights into the folding of knotted proteins in vitro and in vivo. *J. Mol. Biol.* 427:248–258.
16. Mallam, A. L., J. M. Rogers, and S. E. Jackson. 2010. Experimental detection of knotted conformations in denatured proteins. *Proc. Natl. Acad. Sci. USA.* 107:8189–8194.
17. Mallam, A. L., and S. E. Jackson. 2006. Probing nature's knots: the folding pathway of a knotted homodimeric protein. *J. Mol. Biol.* 359:1420–1436.
18. Mallam, A. L., S. C. Onuoha, …, S. E. Jackson. 2008. Knotted fusion proteins reveal unexpected possibilities in protein folding. *Mol. Cell.* 30:642–648.
19. Noel, J. K., J. N. Onuchic, and J. I. Sulkowska. 2013. Knotting a protein in explicit solvent. *J. Phys. Chem. Lett.* 4:3570–3573.
20. Mallam, A. L., and S. E. Jackson. 2011. Knot formation in newly translated proteins is spontaneous and accelerated by chaperonins. *Nat. Chem. Biol.* 8:147–153.
21. Virnau, P., L. A. Mirny, and M. Kardar. 2006. Intricate knots in proteins: function and evolution. *PLoS Comput. Biol.* 2:e122.
22. Taylor, W. R. 2007. Protein knots and fold complexity: some new twists. *Comput. Biol. Chem.* 31:151–162.
23. Sułkowska, J. I., P. Sulkowski, …, M. Cieplak. 2008. Stabilizing effect of knots on proteins. *Proc. Natl. Acad. Sci. USA.* 105:19714–19719.
24. Wagner, J. R., J. S. Brunzelle, …, R. D. Vierstra. 2005. A light-sensing knot revealed by the structure of the chromophore-binding domain of phytochrome. *Nature.* 438:325–331.
25. Lim, K., H. Zhang, …, O. Herzberg. 2003. Structure of the YibK methyltransferase from Haemophilus influenzae (HI0766): a cofactor bound at a site formed by a knot. *Proteins.* 51:56–67.
26. Dabrowski-Tumanski, P., A. Stasiak, and J. I. Sulkowska. 2016. In search of functional advantages of knots in proteins. *PLoS One.* 11:e0165986.
27. Hess, B., C. Kutzner, …, E. Lindahl. 2008. GROMACS 4: algorithms for highly efficient, load-balanced, and scalable molecular simulation. *J. Chem. Theory Comput.* 4:435–447.

28. MacKerell, A. D., D. Bashford, …, M. Karplus. 1998. All-atom empirical potential for molecular modeling and dynamics studies of proteins. *J. Phys. Chem. B.* 102:3586–3616.
29. Mackerell, A. D., Jr., M. Feig, and C. L. Brooks, III. 2004. Extending the treatment of backbone energetics in protein force fields: limitations of gas-phase quantum mechanics in reproducing protein conformational distributions in molecular dynamics simulations. *J. Comput. Chem.* 25:1400–1415.
30. Jorgensen, W. L., J. Chandrasekhar, …, M. L. Klein. 1983. Comparison of simple potential functions for simulating liquid water. *J. Chem. Phys.* 79:926–935.
31. Darden, T., D. York, and L. Pedersen. 1993. Particle mesh Ewald: an N•log(N) method for Ewald sums in large systems. *J. Chem. Phys.* 98:10089–10092.
32. Bennion, B. J., and V. Daggett. 2003. The molecular basis for the chemical denaturation of proteins by urea. *Proc. Natl. Acad. Sci. USA.* 100:5142–5147.
33. Mallam, A. L., and S. E. Jackson. 2007. A comparison of the folding of two knotted proteins: YbeA and YibK. *J. Mol. Biol.* 366:650–665.
34. Mayor, U., C. M. Johnson, …, A. R. Fersht. 2000. Protein folding and unfolding in microseconds to nanoseconds by experiment and simulation. *Proc. Natl. Acad. Sci. USA.* 97:13518–13522.
35. Rocco, A. G., L. Mollica, …, I. Eberini. 2008. Characterization of the protein unfolding processes induced by urea and temperature. *Biophys. J.* 94:2241–2251.
36. Wang, Q., A. Christiansen, …, M. S. Cheung. 2011. Comparison of chemical and thermal protein denaturation by combination of computational and experimental approaches. II. *J. Chem. Phys.* 135:175102.
37. Vega, C., and J. L. Abascal. 2011. Simulating water with rigid nonpolarizable models: a general perspective. *Phys. Chem. Chem. Phys.* 13:19663–19688.
38. He, C., G. Lamour, …, H. Li. 2014. Mechanically tightening a protein slipknot into a trefoil knot. *J. Am. Chem. Soc.* 136:11946–11955.
39. Bornschlögl, T., D. M. Anstrom, …, K. T. Forest. 2009. Tightening the knot in phytochrome by single-molecule atomic force microscopy. *Biophys. J.* 96:1508–1514.
40. Humphrey, W., A. Dalke, and K. Schulten. 1996. VMD: visual molecular dynamics. *J. Mol. Graph.* 14:33–38, 27–28..
41. Gront, D., S. Kmiecik, and A. Kolinski. 2007. Backbone building from quadrilaterals: a fast and accurate algorithm for protein backbone reconstruction from alpha carbon coordinates. *J. Comput. Chem.* 28:1593–1597.
42. Gosavi, S., P. C. Whitford, …, J. N. Onuchic. 2008. Extracting function from a β-trefoil folding motif. *Proc. Natl. Acad. Sci. USA.* 105:10384–10389.
43. Sułkowska, J. I., P. Sułkowski, …, M. Cieplak. 2010. Untying knots in proteins. *J. Am. Chem. Soc.* 132:13954–13956.
44. Perilla, J. R., B. C. Goh, …, K. Schulten. 2015. Molecular dynamics simulations of large macromolecular complexes. *Curr. Opin. Struct. Biol.* 31:64–74.
45. Raval, A., S. Piana, …, D. E. Shaw. 2016. Assessment of the utility of contact-based restraints in accelerating the prediction of protein structure using molecular dynamics simulations. *Protein Sci.* 25:19–29.
46. Tsai, J., R. Taylor, …, M. Gerstein. 1999. The packing density in proteins: standard radii and volumes. *J. Mol. Biol.* 290:253–266.
47. Sułkowska, J. I., P. Sułkowski, and J. Onuchic. 2009. Dodging the crisis of folding proteins with knots. *Proc. Natl. Acad. Sci. USA.* 106:3119–3124.
48. Cieplak, M., and J. I. Sułkowska. 2005. Thermal unfolding of proteins. *J. Chem. Phys.* 123:194908.
49. Mallam, A. L. 2009. How does a knotted protein fold? *FEBS J.* 276:365–375.
50. King, N. P., A. W. Jacobitz, …, T. O. Yeates. 2010. Structure and folding of a designed knotted protein. *Proc. Natl. Acad. Sci. USA.* 107:20732–20737.
51. Wang, P., L. Yang, …, X. S. Zhao. 2013. Single-molecule detection reveals knot sliding in TrmD denaturation. *Chemistry.* 19:5909–5916.
52. Marszalek, P. E., and Y. F. Dufrêne. 2012. Stretching single polysaccharides and proteins using atomic force microscopy. *Chem. Soc. Rev.* 41:3523–3534.
53. He, C., G. Z. Genchev, …, H. Li. 2012. Mechanically untying a protein slipknot: multiple pathways revealed by force spectroscopy and steered molecular dynamics simulations. *J. Am. Chem. Soc.* 134:10428–10435.
54. Dzubiella, J. 2013. Tightening and untying the knot in human carbonic anhydrase III. *J. Phys. Chem. Lett.* 4:1829–1833.
55. Jamroz, M., W. Niemyska, …, J. I. Sulkowska. 2015. KnotProt: a database of proteins with knots and slipknots. *Nucleic Acids Res.* 43:D306–D314.
56. Sułkowska, J. I., E. J. Rawdon, …, A. Stasiak. 2012. Conservation of complex knotting and slipknotting patterns in proteins. *Proc. Natl. Acad. Sci. USA.* 109:E1715–E1723.
57. Zhao, Y., M. Chwastyk, and M. Cieplak. 2017. Structural entanglements in protein complexes. *J. Chem. Phys.* 146:225102.
58. Sułkowska, J. I., P. Sułkowski, …, M. Cieplak. 2008. Tightening of knots in proteins. *Phys. Rev. Lett.* 100:058106.
59. Dietz, H., and M. Rief. 2004. Exploring the energy landscape of GFP by single-molecule mechanical experiments. *Proc. Natl. Acad. Sci. USA.* 101:16192–16197.